Journal of the Serbian Chemical Society
JSCS-info@shd.org.rs • www.shd.org.rs/JSCS
J. Serb. Chem. Soc. 80 (4) 529–547 (2015)
JSCS–4736
UDC 678.674:542.92.000.57:547.473.2+546.284:66.017
Original scientific paper

Influence of clay organic modifier on the morphology and performance of poly(ε-caprolactone)/clay nanocomposites

MARIJA S. NIKOLIĆ*#, NATAŠA ĐORĐEVIĆ, JELENA ROGAN# and JASNA ĐONLAGIĆ#

Faculty of Technology and Metallurgy, University of Belgrade, Karnegijeva 4, 11000 Belgrade, Serbia

(Received 24 September, revised 19 November, accepted 20 November 2014)

Abstract: Two series of poly(ε-caprolactone) poly(oxepan-2-one) nanocomposites with different organo-modified clays (1 to 8 wt. %) were prepared by the solution casting method. Organoclays with polar (Cloisite® C30B) and nonpolar (Cloisite® C15A) organic modifiers and with different miscibility with the poly(ε-caprolactone) matrix were chosen. Exfoliated and/or intercalated structures of the nanocomposite were obtained using high dilution and ultrasonic treatment for the preparation of the composite. The effects of the surface modification and clay content on the morphology, and mechanical and thermal properties of the nanocomposites were studied. Scanning electron microscopy excluded the formation of microcomposites. The wide-angle X-ray diffraction analysis revealed that the tendency toward exfoliated structures was higher with Cloisite® C30B, which had better miscibility with poly(ε-caprolactone) matrix, than with Cloisite® C15A. Differences in the sizes of the spherulites and morphology between two series of the nanocomposites were observed by optical microscopy performed on as-cast films. The enthalpies of fusion and degrees of crystallinity were higher for the nanocomposites than for the neat poly(ε-caprolactone) and increased with clay loading in both series, because of the nucleating effect of the clay. The decreased thermal stability of the nanocomposites was ascribed to the thermal instability of the organic modifiers of the clays. The Halpin–Tsai model was used to compare the theoretically predicted values of the Young's modulus with the ones experimentally obtained in tensile tests.

Keywords: biodegradable; aliphatic polyester; layered silicate; solution casting.

INTRODUCTION

Polymer nanocomposites are already established as materials with remarkably enhanced and improved properties compared to the pure polymers and con-

* Corresponding author. E-mail: mnikolic@tmf.bg.ac.rs
# Serbian Chemical Society member.
doi: 10.2298/JSC140924119N

ventional microcomposites. If a very low amount of nanometer filler is successfully dispersed in a polymer matrix, the interface between the filler and the matrix dramatically increases, allowing a full contribution of the filler to the improvement of the properties. Among polymer/inorganic filler composites, polymer/layered silicate nanocomposites have induced a great interest in industry, as well as in academia.[1–4] Layered silicates found such a prominent place among other nanofillers due to their natural abundance, high mechanical strength, chemical resistance and well-investigated intercalation chemistry. Different polymers, such as polyamides, polypropylene, polyurethane, aliphatic polyesters, aimed at diverse applications, were investigated as matrices in polymer/layer silicate nanocomposites. The resulting nanocomposites often exhibit higher stiffness, lower permeability, reduced coefficient of thermal expansion and reduced flammability than the corresponding neat polymer.[4–7]

A layered silicate with a layer thickens of 1 nm and high aspect ratio (10––1000) is organized in stacks with regular gaps between them, called interlayers or galleries. The clay layers are negatively charged with this charge being counterbalanced by alkali or alkaline earth cations that reside in the galleries. In a preparation of polymer/layered silicate nanocomposite, the tendency is to obtain a full, nanometer dispersion of clay layers, *i.e.* exfoliation, in order to achieve the best performance. It was also shown that the intercalation of polymer chains into the interlayer space, resulting in a well-ordered multilayer morphology with a few clay layers in dispersed stacks, can also result in a substantial improvement of material properties.[8,9] The particular structure that is obtained is influenced by the elaboration route and the favorable polymer–clay interactions. Clay is usually modified by exchanging the interlayer inorganic cations with organic ions, which enables more favorable interactions with the desired, usually hydrophobic, matrix. At the same time, the tethering of long alkyl chains to the surface of the layer increases the interlayer spacing, allowing an easier approach of a polymer chain. A range of commercial organoclays is available, intercalated with different organic cations, usually quaternary ammonium ions.

Poly(ε-caprolactone), PCL (poly(oxepan-2-one)) belongs to an important class of biodegradable polymers – aliphatic polyesters. It is a semi-crystalline polymer with low melting and glass transition temperatures. PCL degrades by hydrolytic cleavage of the ester bonds along the polymer chain, yet with a much slower rate compared to those of other aliphatic polyesters, such as poly(L,D--lactic acid). Therefore, when medical applications are in question, this polyester has been investigated for some long-term applications, such as in some prolonged controlled release systems or for different scaffolds, where physical and mechanical properties should be maintained for at least 6 months.[10] In the case of scaffolds in bone tissue engineering, the mechanical properties of PCL might not be adequate for such high-load-bearing applications and therefore need some

improvements. PCL is also considered as a suitable, environmentally friendly replacement for some non-biodegradable commodity polymers that are currently in use, *e.g.*, for packaging or in agriculture. It is, therefore, of considerable interest to investigate and develop improvements of PCL-based materials in terms of mechanical, barrier and thermal properties. Judging from the literature citations, a nanocomposite approach has been especially investigated.[11–15] Nanoclays which provide a range of aforementioned improvements of materials seems to be a particularly promising filler for materials based on a PCL-matrix.[16]

The main elaboration routes to PCL/clay nanocomposites are *in situ* polymerization of the ε-caprolactone monomer intercalated in the clay galleries, melt processing and casting from solution. By *in situ* intercalative polymerization, well-defined exfoliated nanocomposites could be obtained, though high molecular weights of the matrix are not easy to attain.[17–23] A process was also developed in which an exfoliated master batch, prepared by *in situ* polymerization, was dispersed in the desired matrix by melt processing.[24] Melt processing was not so efficient as *in situ* polymerization in achieving exfoliated state, even though it is the simplest and industrially most acceptable route to nanocomposites.[25–30] An important point in melt processing when used for organically modified clay is the thermal stability of the organic modifiers. A number of papers dealing with commercial organoclays presented the influence of the thermal instability of the organic modifier on the final performance of melt processed nanocomposites.[31,32] Early work on the preparation of PCL/clay nanocomposites by solution casting resulted in only slightly intercalated nanocomposites.[33] Unlike poly(lactic acid)/clay nanocomposites, for which solution casting was proved to be a good method for obtaining exfoliated/intercalated and intercalated structures of nanocomposites,[34,35] in the preparation of PCL/clay nanocomposites, this route was not that successful. However, recent reports on PCL/clay composites claimed that an intercalated/exfoliated structure could be achieved by the proper choice of solvent in respect to the clay and PCL and a highly dilute starting suspension.[36] By applying the solution casting method, the danger of thermal degradation of the organic modifier is eliminated. This allows the investigation and better understanding of the impact of interactions between an organic modifier and the PCL matrix on clay dispersion and the final performance of the nanocomposites.[37]

In this report, an attempt to obtain PCL/clay nanocomposites *via* the film casting technique is described. The aim was to explore the influence of organic modifiers on clay dispersion within a PCL matrix. Two organoclays (Cloisite® 30B and Cloisite® 15A), which differ in respect to their affinity toward the used solvent and the PCL matrix, were investigated. The organo-modifier in the case of Cloisite® 30B was the methyl bis-2-hydroxyethyl tallow quaternary ammonium cation and in the case of Cloisite® 15A, the dimethyl dehydrogenated

tallow quaternary ammonium cation (Fig. 1). In addition, the thermal and mechanical properties of the as-prepared samples were investigated and the results interpreted in terms of the achieved clay dispersion and interactions between the clay organic modifier and the matrix.

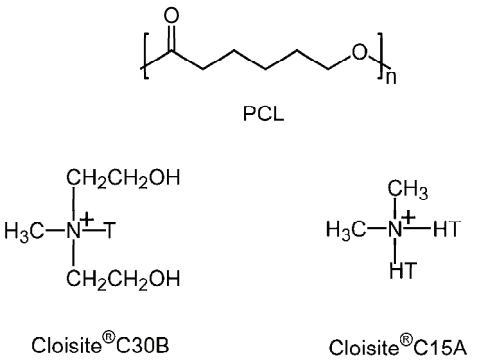

Fig. 1. Chemical structures of PCL and organic modifier of the clays: for Cloisite® 30B methyl bis-2-hydroxyethyl tallow (T) quaternary ammonium cation and for Cloisite® 15A dimethyl dehydrogenated tallow (HT) quaternary ammonium cation (T is tallow (≈65 % C18, ≈30 % C16, ≈5 % C14).

EXPERIMENTAL

Materials

Poly(ε-caprolactone) was synthesized by ring-opening polymerization of ε-caprolactone in the presence of stannous octoate catalyst.[38] The stannous octoate was purchased from Aldrich and used as received. The number average molecular weight of the synthesized PCL was 43300 g mol^{-1} with a polydispersity of 1.95, as obtained from size exclusion chromatography measurements performed in chloroform (solution concentration 10 mg mL^{-1}; mobile phase flow rate 1 mL min^{-1}) with polystyrene calibration. The two organo-modified clays were supplied by Southern Clay Products, Inc. (Texas, USA) under the trade name Cloisite® 30B and Cloisite® 15A (hereafter denoted as C30B and C15A, respectively). The cation exchange capacity (*CEC*) was 90 mmol M^+ 100 g^{-1} for C30B and 125 mmol M^+ 100 g^{-1} for C15A. The organic content of the organo-modified clay was determined by thermogravimetric analysis TGA, *i.e.*, 30 wt. % for C30B and 43 wt% for C15A. All solvents were purchased from Merck and used as received.

Preparation of PCL/organoclay nanocomposites

PCL/organoclay nanocomposites were prepared by a solvent casting method. The compositions of the nanocomposites with used designation of the samples are presented in Table I. Dispersion of clay and a solution of PCL in chloroform were prepared separately. For the clay dispersion (10 mg ml^{-1}), intensive mixing with a magnetic stirrer (1000 s^{-1}) and ultrasonic treatment in two 10 min cycles were applied. A predetermined amount of clay dispersion was added dropwise in the PCL solution and final dispersion was treated in an ultrasonic bath for 15 min, followed by intensive mixing at 1000 s^{-1} on a magnetic stirrer for one hour. The resultant dispersion was poured into Petri dishes and chloroform was allowed to evaporate under atmospheric conditions. The films of around 200 μm thickness were peeled from the dishes and subjected to further analysis.

X-Ray diffraction

Wide-angle X-ray diffraction (WAXD) patterns were recorded on an ItalStructure APD2000 powder diffractometer in a Bragg–Brentano geometry using CuK_α radiation (λ =

= 0.15418 nm) and step–scan mode (range: 3–10° 2θ, step-time: 4 s, step-width: 0.02°). The organoclays were in the form of powder and the nanocomposites were analyzed as obtained in a form of thin flat films. The interlayer mean *d*-spacing of the clays was calculated by means of Bragg's law.

Optical microscopy

The surface of nanocomposite films was observed by an optical microscope Leica DM ILM in reflected light. The spherulites' diameters were measured from obtained microphotographs and given as a mean value calculated from 200 independent measurements.

Scanning electron microscopy

Scanning electron microscopy (SEM) measurements were carried out on a JEOL JSM--6610LV microscope operating at 30 kV acceleration voltage. The surfaces of the as-cast films as well as fractured surfaces of the nanocomposite films were observed. The samples were cryo-fractured in liquid nitrogen and coated with a thin layer of gold prior to the measurements.

Differential scanning calorimetry

Differential scanning calorimetry (DSC) tests were performed on an SDT Q600 (TA instruments, USA) instrument. The samples (around 5 mg) were scanned from 30 to 200 °C at a rate of 10 °C min^{-1} in a nitrogen atmosphere.

Thermogravimetric analysis

Thermogravimetric analysis (TGA) was carried out with an SDT Q600 (TA instruments, USA) instrument by recording the weight loss during the heating of the samples of around 5 mg to 800 °C with a 10 °C min^{-1} heating rate under a nitrogen flow of 0.1 dm^3 min^{-1}.

Tensile properties

The mechanical properties were studied using an AG-Xplus Testing machine (Shimadzu, Japan) at a crosshead speed of 1 mm min^{-1}. The tests were performed on as-obtained samples after solution casting, which were shaped in rectangular form with the dimensions 40 mm×10 mm and thickness of around 200 μm. An average of five measurements was taken for each sample. The samples were conditioned prior to the measurements at 25 °C and 65 % relative humidity for 24 h.

RESULTS AND DISCUSSION

Structural and morphological characterization

The clay dispersion in the nanocomposites was analyzed by wide-angle X-ray diffraction. The WAXD patterns for the pure clays and the corresponding nanocomposites are presented in Fig. 2. The pattern of the PCL matrix is also presented as a baseline to compare the difference between the matrix and the nanocomposites. The mean interlayer spacing in C30B clay, elucidated from (001) plane diffraction at 2θ 4.7° was about 1.88 nm. The absence of a (001) reflection in investigated 2θ region in the diffractograms of the nanocomposites with C30B (Fig. 2a) is a strong indication that the clay was dispersed at a level of a single platelet, or that an intercalated structure with an interlayer spacing greater than 2.94 nm was obtained (as indicated with the asterisk in Fig. 2a). If an intercalated structure is assumed, the increase in the interlayer spacing obtained

for the C30B clay was thus greater than 1.06 nm. The WAXD pattern for the C15A clay, presented in the Fig. 2b exhibits reflections at around 2θ 3.0, 4.2 and 6.9°. As stated by the supplier, the interlayer spacing of the (001) plane (d_{001}) for this type of organically modified clay is 3.15 nm; thus, the corresponding reflection in the WAXD pattern should appear at 3.10° 2θ, just within the measurable range of the instrument, as indicated with the arrow in Fig. 2b. As in the case of the nanocomposites with the C30B clay, the absence of reflections in the WAXD patterns of the nanocomposites implies that the dispersion of the clay in the nanocomposites was either intercalated, with a *d*-spacing greater than 3.15 nm, or exfoliated. Only in the case of nanocomposite PCL/C15A-8, could an intercalated structure be confirmed from the observed shift in the diffraction peak at 2θ 6.9° (1.28 nm) in pristine clay to 2θ 4.5° (1.96 nm) in the nanocomposite. The well pronounced broad diffraction peak at 2θ 4.5° could imply that the clay created a dispersion of stacks with very well defined interlayer distances.[34]

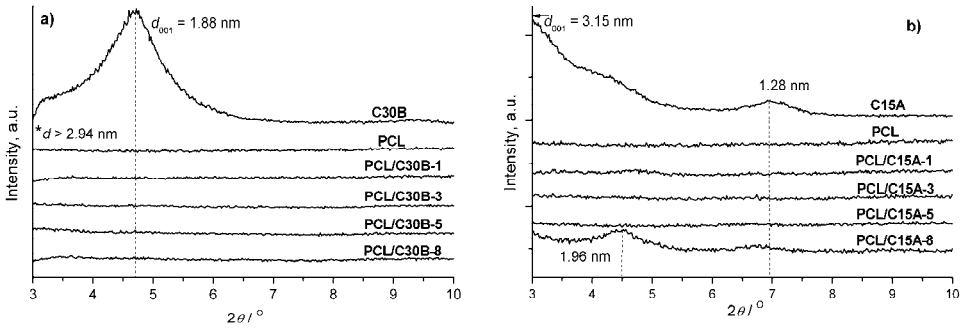

Fig. 2. WAXD patterns for pristine organoclays and the corresponding nanocomposites with a) C30B and b) C15A organoclay.

The nanocomposites reported in the literature prepared by solution casting usually possessed an intercalated structure. Using dichloromethane as a dispersion medium, Ahmed *et al.*[39] obtained an intercalated structure of PCL/C30B nanocomposites unaffected by the clay amount, with a reported interlayer distance increase of 1.14 nm compared to pristine C30B clay, even with the lowest amount of clay (2.5 wt. %). The authors applied the same experimental procedure using the C15A clay; however, no intercalation of PCL into the galleries of this clay was obtained. Ludũena with coworkers reported a mixed exfoliated/intercalated structure of PCL/C30B nanocomposites obtained from dichloromethane and a mixture of dichloromethane/dimethylformamide, judging from the broadening of the diffraction peak in comparison to the clay alone.[40] Neppali reported an intercalated structure for a PCL/C15A nanocomposite prepared from chloroform solution, with an achieved increase in interlayer distance of 0.8 nm.[41] The experimental protocol for the preparation of nanocomposites applied in the pre-

sent study included high dilution of the clay dispersion prior to the addition of this dispersion to the PCL solution. The applied ultrasonic treatment, although not optimized in the term of duration, seems to be well chosen for promoting PCL inclusion into the clay galleries. A similar experimental protocol in terms of high dilution was recently successfully applied for the preparation of exfoliated PCL/clay nanocomposites, even from unmodified clay.[36]

In the elaboration of a solvent casting route, the first thing that must be considered for the achievement of good clay dispersion is the interaction of the solvent with the clay and the polymer. In this study, chloroform was chosen as the dispersion medium being a good solvent for PCL. Moreover, the interaction of chloroform with the two types of clays and its ability to macroscopically swell the clay as well as to increase the interlayer spacing of the clay platelets was thoroughly investigated.[42] Both these parameters, the degree of swelling of the clay in the chloroform (with free swelling factor of 0.5 for C15A and 0.25 for C30B) and the increase in the interlayer spacing in the presence of the solvent, are in favor of C15A, due to the better interactions of the dispersive type of organic modifier of the C15A clay with chloroform. The polarity of the organic modifier of C30B did not provide for good interaction with chloroform. At the same time, the initial basal spacing of C15A (3.15 nm), caused by the tethering of organic ammonium ions on the platelet surface, is higher compared to C30B (1.88 nm). This fact also supports the expectation of better clay dispersion in the polymer matrix in the former case.

However, besides these initial requirements of compatibility of the dispersion medium and blend components, a factor that also influences the final clay dispersion is a good enthalpic interaction between the matrix and the organic modifiers of the clay. The interaction between the organic modifiers and the polymer chain serves to promote the inclusion of the polymer chains in between the clay platelets and to promote exfoliation. As a rough estimation of the interaction of the chosen organic modifiers and PCL, the solubility parameters (δ), calculated by the Hoftyzer–Van Krevelen group contribution method, of the organic modifiers and PCL were compared.[34,43] The δ values: 16.74 for the organic modifier of C15A and 18.73 for organic modifier of C30B in comparison to δ value of 19.44 calculated for the PCL show the better compatibility of PCL and the organic modifier of C30B clay. Thus, from the presented results, it could be concluded that good compatibility between the polymer matrix and the organic modifier of the clay plays the main role in achieving a good clay dispersion, although the process for clay dispersion in the polymer has to be carefully designed.

The surface and cryo-fractured surface morphology of nanocomposite films was observed *via* SEM analysis. Some representative micrographs are presented in Fig. S-1 of the Supplementary material to this paper. The surface of the

as-prepared films was smooth (the micrographs are not presented) without any observable holes, which could be created through fast chloroform evaporation, as previously reported for nanocomposites prepared from low-boiling solvents.[40] However, in the cryo-fractured surfaces, some holes in the sample bulk were registered, which could have an impact on the mechanical properties of the nanocomposites as weak places in the structures. No observable aggregates of the inorganic part of the nanocomposites could be detected by SEM, which is in agreement with the exfoliated/intercalated structure claimed from the WAXD analysis. However, there was a difference in the cryo-fractured surface morphology, which followed the trend of the observed differences in the nanocomposite morphology deduced from WAXD. The fractured surface of PCL was relatively smooth with observable plastic deformations typical for a ductile polymer. With the addition of C30B clay, no change in the cryo-fractured surface morphology was observed. In the case of nanocomposites with higher amount of the C15A clay, large voids and cavities were observable in the cryo-fractured surface. This was especially pronounced for the nanocomposite PCL/C15A-8 with the proven presence of an intercalated morphology. Presumably, the clay stacks present in the PCL/C15A-8 nanocomposite acted as microvoid nucleation sites in this case. The microvoids further grow through debonding between clay and PCL matrix. The smaller interaction between C15A and PCL could possibly favor this process, leading to the formation of many voids. As a result, the coalescence of microvoids leads to the formation of large voids and cavities protruding through the matrix bulk. Fibrillation of the polymer observed for some samples is highly atypical for cryo-fractured surfaces. Some earlier reports on nanocomposites with organically modified clays found that the organic modifier could have a plasticizing effect.[20,44] The possible plasticizing effect of the organic modifier present in the highest amount in PCL/C15A-8 (Table I) could be a reason for the observed fibrillation of the polymer matrix.

TABLE I. Composition of PCL/clay nanocomposites

Sample	Type of clay	PCL content wt. %	Organoclay content[a] wt. %	ϕ_{clay}[b] vol. %
PCL/C30B-1	Cloisite® 30B	99.0	1.0 (0.7)	0.6
PCL/C30B-3		97.0	3.0 (2.2)	1.8
PCL/C30B-5		95.0	5.0 (3.6)	2.9
PCL/C30B-8		92.0	8.0 (5.8)	4.6
PCL/C15A-1	Cloisite® 15A	99.0	1.0 (0.6)	0.7
PCL/C15A-3		97.0	3.0 (1.8)	2.1
PCL/C15A-5		95.0	5.0 (2.9)	3.5
PCL/C15A-8		92.0	8.0 (4.6)	5.5

[a]Values in the brackets refer to inorganic part; [b]the volume fraction of the clay calculated using the following values of the densities of the composite constituents: ρ_{PCL} = 1.2 g cm^{-3}, ρ_{C30B} = 1.98 g cm^{-3}, ρ_{C15A} = 1.66 g cm^{-3}

Thermal properties and crystallization

Melting temperatures and heats of fusion of PCL/clay nanocomposites were probed by DSC analysis. The results of the analysis of the DSC thermograms are summarized in Table II, from which it could be seen that there were no differences (within experimental error) in melting temperatures of the nanocomposites compared to that of the neat matrix. This means that the crystalline lamellae structure was not affected by the presence of the clay. However, marked differences were observed for the heat of fusion of the nanocomposites compared to that of neat PCL. The heats of fusion were determined by integration of the endothermic peak on the DSC thermograms. The values of the enthalpies of fusion of the nanocomposites exhibited differences that follow a similar, increasing trend with the increasing clay content in both series. The degree of crystallinity of the PCL matrix (X_c) in the samples was obtained from the values of enthalpies of fusion, by normalizing them to the PCL content and comparing to the heat of fusion of 100 % crystalline PCL (136.1 J g^{-1}).[19] Judging from obtained values for the degree of crystallinity of the nanocomposites, the amount of the crystalline PCL fraction was increased in the presence of the clay and this enhancement was influenced by the clay content.

TABLE II. Melting temperatures, heats of fusion, degree of crystallinity and spherulite diameters measured for neat PCL and PCL/clay nanocomposites

Sample	T_m[a] / °C	ΔH_m / J g^{-1}	X_c / %	$d_{spherulite}$ / μm
PCL	66	85.2	63	84 ± 12
PCL/C30B-1	66	90.5	67	79 ± 14
PCL/C30B-3	68	98.9	75	–
PCL/C30B-5	66	88.5	69	–
PCL/C30B-8	67	105.4	84	–
PCL/C15A-1	67	85.8	64	73 ± 15
PCL/C15A-3	66	97.0	73	94 ± 20
PCL/C15A-5	67	81.9	63	90 ± 20
PCL/C15A-8	66	95.9	77	92 ± 19

[a]Determined as the temperature of the maximum of the endothermic peak in DSC thermograms

The diameters of spherulites, observed by optical microscopy, are also given in Table II. In the images obtained using optical microscopy (Fig. S-2 of the Supplementary material), no holes or voids could be detected at the surface, as also shown by SEM. In the images of the surface of the nanocomposites formed in contact with a flat glass surface, a developed spherulite structure could be nicely observed. The spherulites structure and their border in neat PCL could be very well captured.

With the addition of the clay, the spherulite structure was severely destroyed with their borders fusing together. The effect was more pronounced in the case of the PCL/C30B nanocomposites, where the spherulite borders were observable

only for the nanocomposite with the lowest amount of clay. The diameter of spherulites decreased from around 84 μm for neat PCL to 79 μm for PCL/C30B-1 and 73 μm for PCL/C15A-1. The decrease in the diameter of the spherulites with increasing clay content, which is very often observed, is a consequence of the nucleating effect of the clay. As a result, the nanocomposites contained a higher number of smaller spherulites with increasing clay content. This trend was obviously continued in the case of the nanocomposites with C30B clay, for which, with increasing clay content, no clear spherulite borders could be distinguished. The change in the morphology of the spherulites can be explained if it is assumed that C30B clay, besides acting as a nucleating agent, disturbs the spherulite radial growth by a network of finely dispersed platelets/tactoids (clay stacks). Simultaneously, samples in PCL/C30B series had higher degrees of crystallinity compared to neat PCL and the nanocomposites containing C15A clay. An increased degree of crystallinity of nanocomposites compared to the matrix polymer is rarely observed in the literature and is explained with the nucleating effect of the clay.[20]

Interestingly, in the case of nanocomposites with C15A clay, an increase in spherulite diameter compared to neat PCL, for clay loadings higher than 1 wt. % was observed. The increase of spherulites in the presence of the clay was reported for poly(L-lactic acid)/clay nanocomposites,[35] albeit in nanocomposites where exfoliation of the clay was achieved, which is quite contrary to the present situation. The highest value of spherulite diameters for presented series of nanocomposites were observed in the case of an intercalated structure. The observed higher diameters of spherulites in the as-cast films might be a consequence of more effective heterogeneous nucleation in the PCL/C15A series, which accelerates the overall process of crystallization from the solution. Thus, the crystallization process was not restricted by the evaporation of the solvent and was accompanied with no disturbances by the silicate layer network. Since a larger portion of the silicate layers is present as tactoids rather than as single platelets, the possibility of network formation was lower or a less dense network was formed. In the case of PCL/C30B nanocomposites, which have a better dispersion of the clay platelets silicates layer network, formed from the single clay platelets, the radial growth of spherulites was disturbed, resulting in a quite different morphology of nanocomposites. In the PCL/C15A series, the degree of crystallinity was higher for nanocomposites in comparison to that of neat PCL, and followed a similar trend to that observed in the PCL/C30B series.

Thermal stability of nanocomposites

Thermal degradation of nanocomposites was investigated in non-isothermal TG experiments under a nitrogen atmosphere at a heating rate of 10 °C min^{-1}. The TG thermograms of PCL and PCL/clay nanocomposites of different compositions are presented in Fig. 3a and b.

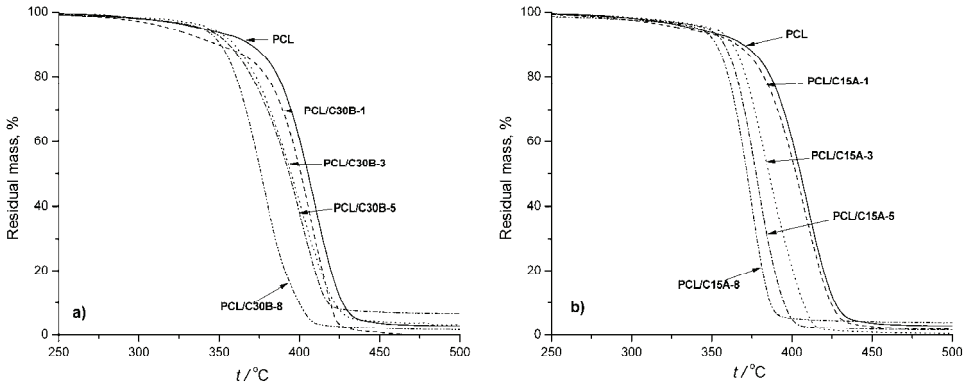

Fig. 3. TG curves obtained in a nitrogen atmosphere at a heating rate of 10 °C min^{-1} for nanocomposites with a) C30B clay and b) C15A clay.

The characteristic temperatures for a mass loss of 3 wt. %, taken as an indication of the beginning of the degradation, and for a mass loss of 50 wt. % are summarized in Table III. The onset temperature of thermal degradation is slightly higher for almost all nanocomposites in comparison to the neat PCL, with the exceptions of the nanocomposites with the lowest amount of both types of the clay. However, after this initial stage, a pronounced decomposition of the nanocomposites occurred with all TG curves shifted to lower temperature values relative to the curve for the matrix polymer. The temperatures of the maximum rate of weight loss, obtained from the corresponding DTG curves (not presented) were shifted to lower temperatures, in a trend that followed the increase in the amount of clay in the nanocomposites. Thus, the nanocomposites were less thermally stable, which was unexpected in comparison to some previous findings where an improvement in thermal stability was observed with the inclusion of clay in a polymer matrix.[18,25,36] On the other hand, there are reports of worsened thermal stability of nanocomposites containing clay.[20,45–47]According to the literature, the observed enhancement in thermal stability of polymer/clay nanocomposites is usually ascribed to the shielding effect of clay layers, which act as a barrier to the gasses and volatile degradation products. Moreover, the clay platelets are considered as heat barriers and obstacles for polymer chain motion, leading to further stabilization.[48] However, the organically modified clays possess organic ions, in an amount of 30 to 40 wt. %, which are more prone to thermal degradation compared to the matrix and could affect the overall degradation process. The thermal degradation of the organoclays occurred between 220 and 450 °C (TG curves not presented) under the applied experimental conditions and was connected with the degradation of the organic modifiers. It could be assumed that the degradation of the organic ions had an accelerating effect on the degradation of the polymer. This was further supported by the trend of thermal

stability decrease with increasing amount of organic modifier present in the nanocomposite. Nanocomposites with the C30B clay had lower thermal stability than the corresponding nanocomposites with the C15A clay, even though the content of organic modifier was higher in the latter case. This could be connected to the different thermal stabilities of the corresponding organic modifiers of C30B and C15A[31] and/or the state of the clay dispersion,[49] which could override the influence of the amount of thermally labile organic ions. The results are consistent with previously reported ones, *i.e.*, that a lower thermal stability was noticed for PCL/C30B due to PCL hydrolysis caused by the presence of hydroxyl groups in the modifier compared to nanocomposites with organoclays whose modifier contained only nonpolar groups.[23]

TABLE III. Characteristic temperatures obtained from the TG and DTG curves of PCL and the PCL/clay nanocomposites

Sample	$T_{3\,\%}$ / °C	$T_{50\,\%}$ / °C	T_{maxDTG} / °C
PCL	319	405	410
PCL/C30B-1	303	401	410
PCL/C30B-3	329	395	403
PCL/C30B-5	320	394	401
PCL/C30B-8	322	376	385
PCL/C15A-1	310	402	407
PCL/C15A-3	330	385	383
PCL/C15A-5	326	377	378
PCL/C15A-8	319	371	374

Mechanical properties of the nanocomposites

The characteristic properties of the as-prepared nanocomposite films were determined from tensile tests.

The results of these experiments, *i.e.*, Young's modulus, stress at break and strain at break are summarized in Table IV.

TABLE IV. Tensile properties of PCL and its nanocomposites; E and E_{m} refer to Young's modulus of the nanocomposite and matrix, respectively

Sample	Young's Modus, MPa	E/E_{m}[a]	Stress at break, MPa	Strain at break, %
PCL	327±21	1	15.0 ±1.1	9.8±0.9
PCL/C30B-1	313±26	0.96	14.4±0.7	9.0±1.0
PCL/C30B-3	339±23	1.04	14.1±0.5	9.3±0.9
PCL/C30B-5	289± 11	0.89	11.7±1.4	7.1±1.2
PCL/C30B-8	332±9	1.02	11.9±0.3	6.2±0.4
PCL/C15A-1	331±13	1.01	13.2±0.6	7.3±0.3
PCL/C15A-3	318±14	0.97	10.3±0.4	4.9±1.1
PCL/C15A-5	352±18	1.08	9.6±0.5	4.3±0.5
PCL/C15A-8	417±12	1.28	9.0±0.3	3.2±0.6

PCL is ductile polymer with moderate values of elastic modulus and high values of strain at break. The usually observed effect of the addition of a filler to a polymer matrix is increased stiffness accompanied with embrittlement. The embrittlement is usually ascribed to the formation of agglomerates, particularly at higher clay loadings, which induce weak places in the nanocomposite structure. A lowering of the strain at break from 700 to 7 % was reported for a PCL nanocomposite with 10 wt. % of organo-modified clay, which was ascribed to agglomerate formation.[25] In the present case, the reason for the measured low absolute values of the strain at break, even at very low clay contents and also for the neat PCL, accompanied with the absence of yielding, probably lies in the structure of the specimens. The specimens used in the tensile tests were as-prepared solution cast films with holes and voids as weak places. However, the addition of clay also contributes to the embrittlement of the material. A trend of decreasing strain at break with increasing clay loading was observed, similar to the usually found embrittlement effect of clay. A distinction could be made between the different clays used; at all compositions, the nanocomposite containing C30B exhibited higher values of the strain at break in comparison to the nanocomposite containing C15A, as a consequence of better clay dispersion, better interaction of organic modifier of C30B with PCL and, consequently, less weak places for the initiation of the cracks.

The values of stress at break were typical for PCL and its nanocomposites reported in the literature. The stress at break followed a similar trend to that of the strain at break, with higher values for the nanocomposites with C30B clay. Analogous argumentation proposed for the trends in the strain at break values probably holds for the observed change in the stress at break values.

The value of the elastic modulus obtained for the PCL matrix was comparable to those hitherto reported for this polyester. Some of the nanocomposites, especially those containing the C30B clay, exhibited lower values of the modulus compared to the PCL matrix. Such unexpected behavior is very rarely reported or explained in the literature. Pentoustier *et al.* reported a decrease in the modulus of a nanocomposite with unmodified clay prepared by *in situ* intercalative polymerization.[18] Ludũena *et al.* observed a reduced modulus relative to the PCL matrix for some nanocomposites prepared by solution casting from dichloromethane or dichloromethane/dimethylformamide.[40] PCL nanocomposites with C15A clay and varying molecular weights of the matrix, studied by Causin *et al.*, showed a reduced modulus in comparison to the neat PCL, in the whole investigated range of clay loadings for nanocomposites prepared by solution casting from tetrahydrofuran.[41,50]

It was interesting to compare the obtained experimental data with theoretical predictions for elastic modulus of nanocomposites with plate-like fillers. The most frequently used Halpin–Tsai Equation was applied to calculate the theo-

retical values for elastic moduli.[50–52] The longitudinal, $E_{\|}$, and transverse, $E_{\perp}$, modulus of Halpin–Tsai model can be expressed by the following equation:

$$\frac{E}{E_{\mathrm{m}}} = \frac{1+\zeta\eta\phi_{\mathrm{filler}}}{1-\eta\phi_{\mathrm{filler}}} \tag{1}$$

where E and E_{m} are the Young's modulus of the composite and matrix, respectively, ϕ_{filler} is the volume fraction of the filler in the nanocomposite and ζ is a shape parameter: $\zeta = 2(l/t)_{\mathrm{filler}}$ for the longitudinal modulus ($E_{\|}$) and $\zeta = 2$ for perpendicular modulus ($E_{\perp}$), where l and t are the length and thickness of the dispersed phase, *i.e.*, clay. The parameter η is defined as:

$$\eta = \frac{(E_{\mathrm{filler}} / E_{\mathrm{m}}) - 1}{(E_{\mathrm{filler}} / E_{\mathrm{m}}) + \zeta} \tag{2}$$

In the case of randomly oriented clay platelets, the equation for the calculation of the modulus is:

$$E = 0.49\, E_{\|} + 0.51\, E_{\perp} \tag{3}$$

In the calculations of the elastic modulus, when good exfoliation could be assumed, single platelets are treated as filler particles or, in the case of intercalated structure, a filler particle is a stack of clay platelets with gallery material. In the case of composites with C30B clay, good exfoliation was assumed and the parameters used for the calculation were $E_{\mathrm{filler}} = E_{\mathrm{clay}} = 178$ GPa[50] and $\phi_{\mathrm{filler}} = \phi_{\mathrm{clay}}$ (Table I). E_{m} was assumed equal to the modulus of the PCL matrix, 327 MPa (Table IV). The calculations were performed for two different aspect ratios of the clay platelets, $l/t = 80$ and 10, and compared to the experimentally observed modulus of the nanocomposite (Fig. 4a). It could be observed that the values predicted by the Halpin–Tsai Model were higher than those experimentally determined and that, even on decreasing the aspect ratio to 10, these corresponding modulus values could not fit to those experimentally determined. It was previously observed that the model cannot accurately predict the E values for particles less than 100 nm in size.[53] Namely, the Halpin–Tsai method does not take into account interfacial molecular structure, which probably played the dominant role for the nanocomposites with particle sizes less than 100 nm.

The second approach, *i.e.*, the intercalated case, was applied for the calculation of the theoretical modulus for the series of nanocomposites with C15A clay. The effective modulus of the filler (a stack of clay platelets in this case) could be approximated by using the rule of mixtures:

$$E_{\mathrm{filler}} = \phi_{\mathrm{platelet}} E_{\mathrm{clay}} + \phi_{\mathrm{gallery}} E_{\mathrm{gallery}} \tag{4}$$

where ϕ_{platelet} and ϕ_{gallery} are the volume fractions of clay platelets and gallery space in the stack, respectively, while E_{clay} and E_{gallery} are the modulus of silicate platelets and the intercalated material in the gallery, respectively. The

volume fraction of clay platelets in the lamellar stacks, $\phi_{platelet}$, was calculated as the ratio of the total thickness of the clay platelet (obtained by multiplying the thickness of a single platelet, $t_{platelet}$, by the number of the platelets per stuck, $n_{platelet}$) and the thickness of the entire lamellar stack (t_{stack}) and could be expressed as follows:

$$\phi_{platelet} = \frac{n_{platelet} t_{platelet}}{t_{stack}} = \frac{t_{platelet}}{d_{001}} \quad (5)$$

Thus, the volume fraction of clay platelets can be calculated by using the thickness of a single platelet (1 nm)[51] and the number of platelets in the stack (which is usually determined from TEM measurements), or by using the *d*-spacing of the nanocomposite determined by WAXD. Here, the literature value of d_{001}=3.63 nm from a similar pattern as in the present case was used.[39] The value of 27.5 vol. % for the volume fraction of silicate platelets, $\phi_{platelet}$, was obtained. A value of 178 GPa was used for the modulus of the silicate platelets. The modulus of the organic interlayer material (organic modifier of C15A and PCL chains) was expected to be significantly smaller than the modulus of the clay platelets. Thus, the contribution of $E_{gallery}$ to the E_{filler} could be neglected. Hence, the calculated modulus of the filler decreased form 178 GPa to 49 GPa, because of the intercalation. In this way, the calculated modulus of the filler was reduced by 72 %. However, there are some reports that the so-obtained modulus is still an overestimation of the real filler modulus.[54]

The intercalation of the clay by PCL will increase the effective volume fraction of the filler. Under the assumption that the effective volume is proportional to the interlayer spacing,[53] the increase in the volume fraction was taken to be equal to the increase in the d_{001}-spacing, which was 1.15 times. Although intercalation was not proven for the nanocomposites with less than 8 wt. % of C15A, all theoretical predictions were also performed for these nanocomposites for the sake of comparison (Fig. 4b).

Based on a comparison of theoretical and experimental nanocomposite modulus, it is clear that the theoretical Halpin–Tasai modulus could approach the experimentally observed values if the aspect ratio of the filler was lowered, in the case of nanocomposites with C15A clay even to a value of $(l/t)_{filler}$= 4. For the nanocomposite PCL/C15A-8, with proven intercalated structure and with d_{001} = = 3.63 nm, which was used for the calculations, the number of platelets per filler stack is greater than 7, if the value of *l* is assumed to be 100 nm. However, as shown in the case of nanocomposites of C30B clay, the value of *l* is possibly lower than 100 nm, which would decrease the number of platelets in the clay stack.

In summary, the Halpin–Tsai Model can better predict the modulus in the case of intercalated nanocomposites obtained with the C15A clay, while for the

exfoliated structure, this model overestimates the modulus as was shown previously for PLA nanocomposites.[53]

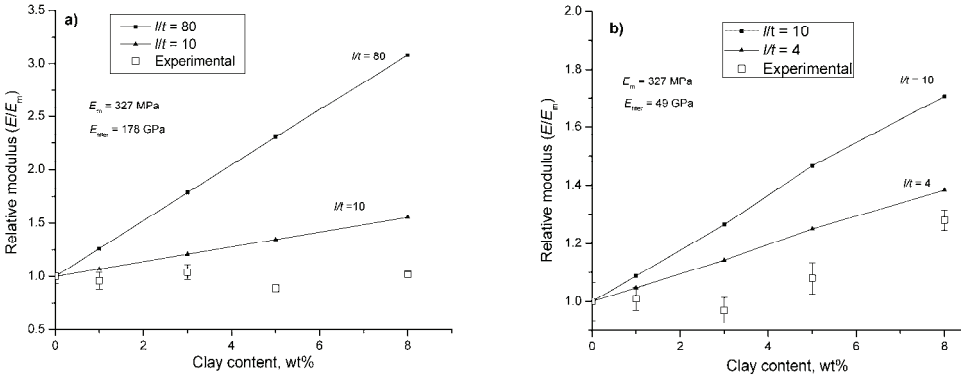

Fig. 4. Comparison of the experimental relative modulus and predictions by the Halpin–Tsai Model for the nanocomposites with a) C30B and b) C15A clay.

CONCLUSIONS

Two series of PCL nanocomposites with organoclays possessing different organic modifiers were prepared from chloroform solution. The conditions of experimental protocol for composite preparation were optimal from the aspect of achieving the best clay dispersion. WAXD and SEM confirmed that exfoliated or exfoliated/intercalated nanocomposite morphology was obtained. The favorable interaction between organic modifier of the clay and PCL is the most important factor that must be optimized in order to achieve the best clay dispersion. The differences in nanocomposite morphology and degree of crystallinity are ascribed to the differences in the dispersion of the clay. The nanocomposites are less thermally stable than the neat PCL. The decreased thermal stability of the nanocomposites is the consequence of the presence of thermally less stable organic ammonium ions, which accelerate the degradation of the matrix. In terms of mechanical properties, despite the good clay dispersion, almost all nanocomposites have reduced values of the characteristic parameters obtained in tensile tests performed on as-prepared films. The strain at break is reduced with the increasing clay loading. The highest modulus was obtained for the nanocomposite with the intercalated structure. For the composites with exfoliated structure, the Halpin–Tsai Model was found to be inappropriate, while for the intercalated composite, the model was able to capture modulus increase with a very low value of the clay "stuck" aspect ratio.

SUPPLEMENTARY MATERIAL

SEM micrographs of the fractured surface of the nanocomposites and images of PCL and PCL/clay nanocomposite films obtained by optical microscopy are available electronically from http://www.shd.org.rs/JSCS/, or from the corresponding author on request.

Acknowledgement. This work was financially supported by the Ministry of Education, Science and Technological Development of the Republic of Serbia (Project No. 172062).

ИЗВОД

УТИЦАЈ ОРГАНСКОГ МОДИФИКАТОРА ГЛИНА НА МОРФОЛОГИЈУ И ПЕРФОРМАНСЕ PCL/ГЛИНА НАНОКОМПОЗИТА

МАРИЈА С. НИКОЛИЋ, НАТАША ЂОРЂЕВИЋ, ЈЕЛЕНА РОГАН и ЈАСНА ЂОНЛАГИЋ

Технолошко–металуршки факултет, Универзитет у Београду, Карнегијева 4, 11000 Београд

Припремљене су две серије нанокомпозита на бази поли(ε-капролактона) и две врсте органомодификованих глина, различитих састава (1 до 8 мас. %), методом из раствора. Одабране органомодификоване глине поседују поларни (Cloisite® C30B) и неполарни (Cloisite® C15A) органски модификатор и разликују се по мешљивости са полимерном матрицом. Велико разблажење и третман ултразвуком, коришћени у поступку припреме омогућили су добијање нанокомпозита са ексфолираном и ексфолираном/интеркаларном структуром. Испитиван је утицај модификације и садржаја глина на морфологију, механичка и термичка својства нанокомпозита. Скенирајућом електронском микроскопијом је утврђено да нису добијени микрокомпозити. Дифракцијом рендгенских зрака на великим угловима је утврђено да се боља дисперзија постиже код нанокомпозита са оном глином (Cloisite® C30B) чији органски модификатори имају бољу интеракцију са полимерном матрицом. Оптичком микроскопијом је уочено да филмови добијених нанокомпозита имају сферулите различите величине и морфологије. Промене енталпије топљења и степени кристалиничности су већи код нанокомпозита у односу на чисту матрицу и имају растући тренд са повећањем удела глине у обе серије, што је последица дејства наноглина као центара за нуклеацију. Мања термичка стабилност нанокомпозита у односу на чисту матрицу је приписана термичкој нестабилности самих органских модификатора. Вредности модула еластичности, добијене у тестовима истезања, су упоређене са теоријски прорачунатим према Halpin–Tsai моделу.

(Примљено 24. септембра, ревидирано 19. новембра, прихваћено 20. новембра 2014)

REFERENCES

1. D. R. Paul, L. M. Robeson, *Polymer* **49** (2008) 3187
2. S. Sinha Ray, M. Okamoto, *Prog. Polym. Sci.* **28** (2003) 1539
3. M. Alexandre, P. Dubois, *Mater. Sci. Eng. R* **28** (2000) 1
4. S. Pavlidou, C. D. Papaspyrides, *Prog. Polym. Sci.* **33** (2008) 1119
5. M. A. Tasdelen, *Eur. Polym. J.* **47** (2011) 937
6. B. Chen, J. R. G. Evans, *Macromolecules* **39** (2005) 747
7. G. Gorrasi, M. Tortora, V. Vittoria, E. Pollet, B. Lepoittevin, M. Alexandre, P. Dubois, *Polymer* **44** (2003) 2271
8. E. Manias, A. Touny, L. Wu, K. Strawhecker, B. Lu, T. C. Chung, *Chem. Mater.* **13** (2001) 3516
9. S. Sinha Ray, K. Okamoto, M. Okamoto, *Macromolecules* **36** (2003) 2355

10. M. A. Woodruff, D. W. Hutmacher, *Prog. Polym. Sci.* **35** (2010) 1217
11. Y. Li, C. Han, J. Bian, X. Zhang, L. Han, L. Dong, *Polym. Compos.* **34** (2013) 131
12. N. Moussaif, S. Irusta, C. Yagüe, M. Arruebo, J. G. Meier, C. Crespo, M. A. Jimenez, J. Santamaría, *Polymer* **51** (2010) 6132
13. K. K. Gupta, A. Kundan, P. K. Mishra, P. Srivastava, S. Mohanty, N. K. Singh, A. Mishra, P. Maiti, *Phys. Chem. Chem. Phys.* **14** (2012) 12844
14. R. Augustine, H. Malik, D. Singhal, A. Mukherjee, D. Malakar, N. Kalarikkal, S. Thomas, *J. Polym. Res.* **21** (2014) 347
15. I. Armentano, M. Dottori, E. Fortunati, S. Mattioli, J. M. Kenny, *Polym. Degrad. Stability* **95** (2010) 2126
16. P. Bordes, E. Pollet, L. Averous, *Prog. Polym. Sci.* **34** (2009) 125
17. B. Lepoittevin, N. Pantoustier, M. Devalckenaere, M. Alexandre, D. Kubies, C. Calberg, R. Jérôme, P. Dubois, *Macromolecules* **35** (2002) 8385
18. N. Pantoustier, B. Lepoittevin, M. Alexandre, P. Dubois, D. Kubies, C. Calberg, R. Jérôme, *Polym. Eng. Sci.* **42** (2002) 1928
19. A. Kiersnowski, J. S. Gutmann, J. Pigłowski, *J. Polym. Sci., Polym. Phys.* **45** (2007) 2350
20. K. Chrissafis, G. Antoniadis, K. M. Paraskevopoulos, A. Vassiliou, D. N. Bikiaris, *Compos. Sci. Technol.* **67** (2007) 2165
21. R. Pucciariello, V. Villani, L. Guadagno, V. Vittoria, *J. Polym. Sci., Polym. Phys.* **44** (2006) 22
22. N. Pantoustier, M. Alexandre, P. Degée, C. Calberg, R. Jérôme, C. Henrist, R. Cloots, A. Rulmont, P. Dubois, *e-Polymers* **1** (2001) 77
23. A. Harrane, M. Belbachir, *Macromol. Symp.* **247** (2007) 379
24. J. Kotek, D. Kubies, J. Baldrian, J. Kovářová, *Eur. Polym. J.* **47** (2011) 2197
25. B. Lepoittevin, M. Devalckenaere, N. Pantoustier, M. Alexandre, D. Kubies, C. Calberg, R. Jérôme, P. Dubois, *Polymer* **43** (2002) 4017
26. Y. Di, S. Iannace, E. Di Maio, L. Nicolais, *J. Polym. Sci., Polym. Phys.* **41** (2003) 670
27. I. Janigová, F. Lednický, D. J. Mošková, I. Chodák, *Macromol. Symp.* **301** (2011) 1
28. S. Labidi, N. Azema, D. Perrin, J.-M. Lopez-Cuesta, *Polym. Degrad. Stab.* **95** (2010) 382
29. D. Homminga, B. Goderis, I. Dolbnya, G. Groeninckx, *Polymer* **47** (2006) 1620
30. L. Ludueña, A. Vázquez, V. Alvarez, *J. Comp. Mat.* **46** (2012) 677
31. L. N. Ludueña, J. M. Kenny, A. Vasquez, V. A. Alvarez, *Mater. Sci. Eng., A* **529** (2011) 215
32. L. N. Ludueña, A. Vázquez, V. A. Alvarez, *J. Appl. Polym. Sci.* **128** (2013) 2648
33. G. Jimenez, N. Ogata, H. Kawai, T. Ogihara, *J. Appl. Polym. Sci.* **64** (1997) 2211
34. V. Krikorian, D. J. Pochan, *Chem. Mater.* **15** (2003) 4317
35. V. Krikorian, D. J. Pochan, *Macromolecules* **37** (2004) 6480
36. T. Wu, T. Xie, G. Yang, *Appl. Clay Sci.* **45** (2009) 105
37. F. Clegg, C. Breen, *Appl. Clay Sci.* **85** (2013) 80
38. S. A. Papadimitriou, G. Z. Papageorgiou, D. N. Bikiaris, *Eur. Polym. J.* **44** (2008) 2356
39. J. Ahmed, R. Auras, T. Kijchavengkul, S. K. Varshney, *J. Food Eng.* **111** (2012) 580
40. L. N. Ludueña, V. A. Alvarez, A. Vazquez, *Mater. Sci. Eng.* **460–461** (2007) 121
41. R. Neppalli, V. Causin, C. Marega, R. Saini, M. Mba, A. Marigo, *Polym. Eng. Sci.* **51** (2011) 1489
42. D. Burgentzle, J. Duchet, J. F. Gerard, A. Jupin, B. Fillon, *J. Colloid Interface Sci.* **278** (2004) 26
43. D. W. Van Krevelen, *Properties of the polymers*, Elsevier, Amsterdam, 1976.

44. W. Xie, J. M. Hwu, G. J. Jiang, T. M. Buthelezi, W.-P. Pan, *Polym. Eng. Sci.* **43** (2003) 214
45. J.-H. Chang, Y. U. An, G. S. Sur, *J. Polym. Sci., Polym. Phys.* **41** (2003) 94
46. D. S. Dlamini, S. B. Mishra, A. K. Mishra, B. B. Mamba, *J. Inorg. Organomet. Polym. Mater.* **21** (2011) 229
47. M. S. S. B. Monteiro, C. L. Rodrigues, R. P. C. Neto, M. I. B. Tavares, *J. Nanosci. Nanotech.* **12** (2012) 7307
48. A. Leszczyńska, J. Njuguna, K. Pielichowski, J. R. Banerjee, *Thermochim. Acta* **453** (2007) 75
49. G.-X. Chen, J.-S. Yoon, *Polym. Degrad. Stability* **88** (2005) 206
50. T. D. Fornes, D. R. Paul, *Polymer* **44** (2003) 4993
51. J. I. Weon, H. J. Sue, *Polymer* **46** (2005) 6325
52. K. C. Yung, J. Wang, T. M. Yue, *J. Reinf. Plast. Compos.* **25** (2006) 847
53. S.-M. Lai, S.-H. Wu, G.-G. Lin, T.-M. Don, *Eur. Polym. J.* **52** (2014) 193
54. M. W. Spencer, L. Cui, Y. Yoo, D. R. Paul, *Polymer* **51** (2010) 1056.